A path toward a new generation of sustainable spark ignition engines: Experimental investigations on the synergic use of dual diluted combustion and renewable fuels

Transportation Engineering 20 (2025) 100317

Contents lists available at ScienceDirect

Transportation Engineering

journal homepage: www.sciencedirect.com/journal/transportation-engineering

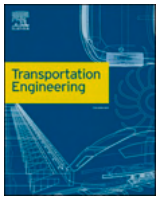

A path toward a new generation of sustainable spark ignition engines: Experimental investigations on the synergic use of dual diluted combustion and renewable fuels

Toni Tahtouh [a], Mathieu André [a], Giuseppe Castellano [b], Luciano Rolando [b,*], Federico Millo [b]

[a] IFP Energies Nouvelles - Institut Carnot IFPEN TE, 1 et 4 avenue de Bois-Préau, 92852 Rueil-Malmaison Cedex, France
[b] Politecnico di Torino - Dipartimento di Energetica, corso Duca degli Abruzzi 24, 10129 Torino, Italy

ARTICLE INFO

Keywords:
Lean combustion
High efficiency spark ignition engine
CO_2 reduction
EURO7
E85

ABSTRACT

Nowadays, the most effective way to tackle the urgent demand for sustainable mobility is the fast development of a wide portfolio of powertrain solutions featuring a low carbon footprint. The PHOENICE (PHev towards zerO EmissioNs & ultimate ICE efficiency) H2020 project aims to demonstrate that highly efficient, low-emitting Internal Combustion Engines (ICEs) remain a viable solution to reduce the environmental impact of road vehicles. This paper presents the results of an extensive experimental campaign on the PHOENICE engine concept which exploits the synergistic combination of homogeneous lean combustion, Exhaust Gas Recirculation (EGR), high compression ratio and aggressive cycle Millerization. The study details the sensitivities on fuel injection, intake valve timing and combustion dilution to assess their impact on fuel conversion efficiency and engine-out emissions. The engine was tested in three combustion modes, achieving a peak Brake Thermal Efficiency (BTE) of 38 % and a broad operating range above 34 % under stoichiometric conditions. EGR provided a maximum relative efficiency gain of 4.2 %, while the combination of EGR and lean combustion yielded to an additional 4.6 % gain with a peak Indicated Thermal Efficiency (ITE) of 47 %. Compared to the baseline engine, the PHOENICE concept reduced Brake Specific Fuel Consumption (BSFC) by at least 10 % over a substantial portion of the engine map. Furthermore, this study explored the fuel economy potential of E85, a renewable blend containing 85 % bioethanol and 15 % gasoline. Results showed up to a 16 % reduction in BSFC in the low-end torque region, largely due to the fuel high knock resistance.

1. Introduction

The growing concern about greenhouse gas emissions and fossil fuel dependency in the transportation sector has become a pivotal topic for both individuals and regulatory authorities. As part of the 'Fit for 55' package [1,2], the European Commission introduced new regulations

Abbreviation: 1D-CFD, One-Dimensional Computational Fluid-Dynamics; AFR, Air-Fuel Ratio; ASC, Ammonia Slip Catalyst; aTCDf, After Top Dead Center of Firing; BD10–90, Combustion duration in crank angles for the mass fraction burned to progress from 10 % (MFB10) to 90 % (MFB90); BMEP, Brake Mean Effective Pressure; BSFC, Brake Specific Fuel Consumption; bTDCf, Before Top Dead Center of Firing; BTE, Brake Thermal Efficiency; CA, Crank Angle; CFD, Computational Fluid-Dynamics; CoV, Coefficient of Variance; CR, Compression Ratio; C-SUV, C-Segment Sport Utility Vehicle; DDCA, Dual Dilution Combustion Approach; DoE, Design Of Experiment; E10, Reference fuel: gasoline with a maximum ethanol content of 10 % by volume; E85, Blend consisting of 85 % bioethanol and 15 % of pure gasoline by volume; EATS, Exhaust After-Treatment System; ECU, Engine Control Unit; EGR, Exhaust Gas Recirculation; EHC, Electrically Heated Catalyst; EIVC, Early Intake Valve Closing; FIS, Fuel Injection System; FMEP, Friction Mean Effective Pressure; GDI, Gasoline Direct Injection; GPF, Gasoline Particulate Filter; ICE, Internal Combustion Engine; IMEP, Indicated Mean Effective Pressure; ITE, Indicated Thermal Efficiency; IVC, Intake Valve Closing; IVO, Intake Valve Opening; LDV, Light-Duty Vehicle; LHV, Lower Heating Value; LIVC, Late Intake Valve Closing; MFB50, Crank Angle degrees corresponding to 50 % of the burnt mass fraction; NMHC, Non-Methane Hydrocarbons; NMOG, Non-Methane Organic Gases; OFAT, One-Factor At a Time; PHEV, Plug-in Hybrid Electric Vehicle; PHOENICE, PHev towards zerO EmissioNs & ultimate ICE efficiency; PM, Particulate Matter; PMEP, Pumping Mean Effective Pressure; PN, Particle Number; P_{rail}, Fuel Rail Pressure; RCP, Rapid Control Prototyping; RON, Research Octane Number; RPM, Revolutions Per Minute; SCR, Selective Catalytic Reduction catalyst; SI, Spark Ignition; SOI, Start Of Injection; TWC, Three-Way Catalyst; VNT, Variable Nozzle Turbine; VVA, Variable Valve Actuation.

* Corresponding author.
E-mail address: luciano.rolando@polito.it (L. Rolando).

https://doi.org/10.1016/j.treng.2025.100317
Received 23 October 2024; Received in revised form 23 January 2025; Accepted 2 March 2025
Available online 4 March 2025

aiming to establish more stringent CO_2 emission standards for new cars and vans. These rules seek to achieve a minimum 55 % reduction in tank-to-wheel CO_2 emissions from light-duty vehicles by 2030, compared to the levels recorded in 1990. In parallel, the preparation for Euro 7 regulation [3] has culminated in an initial agreement between the European Council and Parliament that sets new limits on key pollutants such as NOx and particulate matter, alongside more rigorous testing procedures to ensure compliance under real driving conditions [4].

Addressing these challenges requires the development of multiple sustainable powertrain solutions, rather than relying on a single technology. A comprehensive approach combining renewable energy vectors, such as green electricity, green hydrogen, and renewable fuels, with highly efficient traction systems which have to include electric powertrains as well as hybrid-oriented Internal Combustion Engines (ICE), is essential to address global environmental challenges, promoting energy diversification, and ensuring competitiveness in the European market [5,6].

Within this framework, the PHOENICE project (PHev towards zerO EmissioNs & ultimate ICE efficiency), an EU Horizon2020 initiative, aims at demonstrating that a new generation of efficient, low-emission internal combustion engines can still play a crucial role in reducing the carbon footprint of road transportation. The project focuses on developing a C SUV-class Plug-In Hybrid Vehicle (PHEV) demonstrator, targeting a 10 % improvement in fuel economy compared to the current baseline vehicle available on the market. Furthermore, the vehicle will be fully compliant with the upcoming EU7 regulations achieving the emission standards set by the European Commission Horizon Prize for the Cleanest Engine of the Future [7–9].

To meet these ambitious goals, it is essential to properly identify the technologies capable to overcome the typical limitations of downsized and turbocharged spark-ignition engines. For instance, He et al. [10] developed a stoichiometric gasoline engine with an aggressive Late Miller cycle, high compression ratio, and two-stage turbocharging, achieving a 6 % reduction in Brake Specific Fuel Consumption (BSFC) over the baseline engine. In the context of Gasoline Direct Injection (GDI) engines characterized by high compression ratios, Meng et al. [11] demonstrated that the enhancement of the spray atomization and the high flexibility in the number of injections are critical factors for mitigating knock and optimizing the mixture formation. Meanwhile, Osborne et al. [12] demonstrated that a lean-homogeneous combustion system could achieve more than 10 % BSFC benefits with respect to pure stoichiometric operations and a peak Brake Thermal Efficiency (BTE) of 42 %, being also compliant with NOx emissions limits under real driving conditions. Similarly, Martinez et al. [13] demonstrated a 10 % improvement in fuel conversion efficiency using lean operation on an optical GDI engine and reported low CO emissions, with promising results for particulate and NOx emissions as well. Cooled Exhaust Gas Recirculation (EGR) is another widely used strategy in turbocharged ICEs to control the mixture reactivity and reduce combustion temperatures. Tornatore et al. [14] highlighted the benefits of EGR, particularly at low loads where it reduced pumping losses and improved fuel consumption. At higher loads, EGR provided marginal fuel efficiency gains but significantly reduced NOx emissions with a minor increase in unburned hydrocarbons. However, charge dilution combined with, for instance, Early Miller cycle can negatively impact on the in-cylinder flow motion, reducing the flame propagation speed and the combustion efficiency [15]. To tackle these challenges, Gautrot et al. [16,17] proposed the Swumble™ concept, a combination of tumble and swirl flow structures achieved by redesigning the combustion chamber and intake ducts. This innovative charge motion enhances turbulent kinetic energy with minimal flow capacity degradation, making it particularly well suited to early and late intake valve closing strategies with high dilution rates and high compression ratios.

Furthermore, there is significant potential to improve well-to-wheel CO_2 emissions when advanced engine concepts are combined with renewable fuels. For example, ethanol has been demonstrated to enhance engine performance while simultaneously reducing emissions, as it can be produced using energy sources with a low carbon footprint. Köten et al. [18] found that increasing the ethanol ratio in gasoline blends using a naturally aspirated, single-cylinder, spark ignition engine reduced CO and THC emissions, though NOx emissions rose due to ethanol higher flame speed and higher O_2 content. Farzam et al. [19] demonstrated by numerical simulations that ethanol blends like E25 and E85 can improve the performance of a turbocharged spark-ignition engine, while Singh et al. [20] found that multiple injection strategies with E85 significantly reduced particulate number, total hydrocarbons, and CO emissions, alongside a modest gain in BTE. Lavoie et al. [21] further explored both numerically and experimentally the knock resistance benefits of ethanol in high compression ratio engines. Finally, Krämer and Send [22] evaluated gaseous and particulate emissions of fuels with increasing renewable content, including intermediate ethanol blends (E20, E25), on WLTC and RDE cycles. Balanced ethanol content was shown to reduce CO_2 and maintain low particulate emissions under dynamic conditions, supporting renewable fuels as effective drop-in solutions.

In such a framework, this paper aims at analyzing the performance of an innovative engine concept combining in a synergistic way all the above-mentioned technologies and paving the way for a new generation of environmental-friendly spark ignition engines. More in details, it specifically focuses on the steady-state testing and optimization of the PHOENICE dual-dilution combustion concept, which integrates homogeneous lean combustion with high levels of cooled low-pressure EGR, combined with high compression ratio and aggressive Miller cycle timing. The final objective is to assess the potential of these synergistic technologies in achieving significant reductions in fuel consumption and engine-out emissions.

Following an introduction to the engine architecture and experimental setup, the paper will discuss the experimental investigation, with particular emphasis on how late Miller strategies and dual charge dilution are employed to enhance energy conversion efficiency while minimizing pollutants formation. The subsequent section will present the main engine performance maps for three distinct combustion modes, along with an analysis of the operational constraints impacting full-load performance. In addition, the study will examine the fuel economy potential of E85, a renewable fuel blend composed of 85 % bioethanol and 15 % gasoline. The paper will conclude by summarizing key findings and offering insights into future project activities.

2. Dual dilution engine concept

The PHOENICE concept relies on a state-of-the-art 4-cylinder 1.3L turbocharged direct injection spark ignition engine [23] featuring a high stroke-to-bore ratio, a compact 4-valve combustion chamber with side 200 bar fuel injection system, a MultiAir Variable Valve Actuation (VVA) system [24] and a cylinder head with integrated exhaust manifold. As can be seen from Fig. 1, the project upgrades focused on the engine combustion system, which was re-designed with the target of

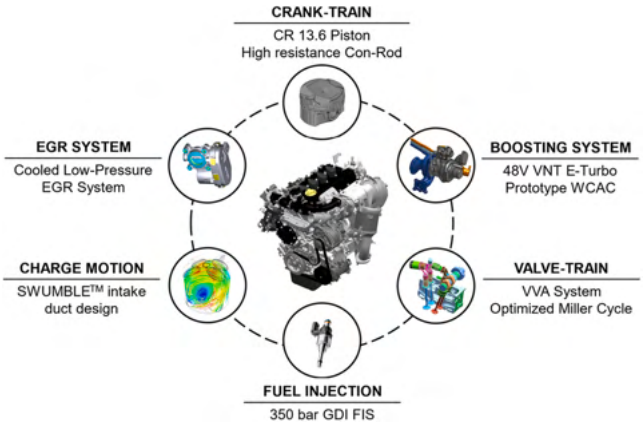

Fig. 1. Innovative technologies considered for PHOENICE prototype engine.

achieving a peak Indicated Thermal Efficiency (ITE) of 47 % exploiting a Dual-Dilution Combustion Approach (DDCA), which combines homogeneous lean mixture with cooled low-pressure EGR, and a high Compression Ratio (CR). These upgrades included the development of a new cylinder head with re-designed intake ducts, the adoption of an electrified turbocharger embedding a Variable Nozzle Turbine (VNT), the installation of a 350 bar capable Fuel Injection System (FIS) and the use of high resistance connecting rods.

Since the flame propagation in such challenging operating conditions should be supported by high levels of turbulence, the intake ports geometry and the piston surface were redesigned to implement the Swumble™ concept previously mentioned in the paper introduction. Previous work by the authors demonstrated that this system could increase average turbulent kinetic energy by approximately 50 % within the spark timing window, based on 3D-CFD cold flow simulations of a part-load operating point [7]. Moreover, the CR was increased up to 13.6 through a new piston design and it was combined with aggressive Miller strategies enabled by the MultiAir system to limit the knock tendency and to reduce the pumping losses at high and low load, respectively. New prototype connecting rods, designed to withstand the elevated in-cylinder pressures resulting from the high compression ratio and dual dilution combustion, replaced the reference components and were integrated into the engine assembly. The charging system was also upgraded with a 48V electrified turbocharger equipped with a Variable Nozzle Turbine (VNT). The aerodynamic specifications of this turbocharger were optimized in previous work by the authors [7,25] to meet the stringent requirements of the designed combustion system. The electric machine integrated into the central housing of the turbocharger not only minimizes time-to-boost but also enables energy recovery when the turbine generates excess power beyond the compressor demand. Finally, the FIS was upgraded with a new pump and new injectors capable to operate up to 350 bar. The combination of all these technologies led to the specifications summarized in Table 1. The maximum load target for this engine was determined through vehicle numerical simulations [9]. Performance benchmarks were set to ensure that the PHOENICE vehicle met state-of-the-art standards. Consequently, the engine specific target was to achieve a Brake Mean Effective Pressure (BMEP) of 20.0 bar and approximately 100 kW of peak power.

The achievement of EU7-compliant tailpipe emissions levels needs an Exhaust After-Treatment System (EATS) specifically tailored for the PHOENICE engine requirements. It is composed by two sections. The close-coupled section comprises an Electrically Heated Catalyst (EHC) and a Three-Way Catalyst (TWC) device to control CO, HC and NOx gaseous emissions under cold-start and stoichiometric ($\lambda = 1$) conditions. Furthermore, a coated Gasoline Particulate Filter (GPF) is used to trap particulate matter. To meet the demanding PN emissions limits prescribed by EU7, an innovative coating technology was used to deliver a step gain in filtration efficiency over the current EU6d-level technologies with an equivalent penalty in backpressure [26]. The underfloor section includes a Selective Catalyst Reduction (SCR) system to convert NOx under lean ($\lambda >$ 1) conditions. Its conversion efficiency at low temperature is further enhanced by an upstream oxidation catalyst (NO—Ox) which converts a portion of the NO into NO_2. Finally, an Ammonia-Slip Catalyst (ASC) is integrated downstream to abate NH_3 slip which may otherwise result from urea overdosing or as a by-product of the reactions in the upstream catalyst devices under stoichiometric operating conditions.

Table 1
PHOENICE engine specifications.

N° of Cylinders	4 In-line
Displacement	1332 cm^3
Bore x Stroke	70 mm x 86.5 mm
Stroke/Bore Ratio	1.24
Compression Ratio	13.6:1
N° of valves	16
VVA system	MultiAir II (intake only)
Turbocharging	48V VNT E-Turbo
Fuel Injection	GDI – up to 350 bar
Ignition System	Normal Production
EGR System	Cooled Low Pressure (LP)
Fuel	E10 – EU6cert
Rated Power (target)	100 kW @ 4500 RPM
Rated Torque (target)	218 Nm @ 3500 RPM

3. Steady-State engine testing

3.1. Experimental setup

The PHOENICE prototype engine was tested at IFPEN facilities on the multi-cylinder engine dynamometer test bench shown in Fig. 2.

Thermocouples and low frequency pressure transducers were installed in the air and EGR loops, in the exhaust line and in both the high and low temperature cooling circuits at the measurement points shown in Fig. 3, to monitor the main engine components and subsystems. The cylinder head was also instrumented with four KISTLER 6052C piezoelectric high frequency pressure transducers allowing an on-line combustion diagnostic for each cylinder. An exhaust gas analyzer was also used to measure gaseous emissions and particulate matter down to 10 nm size. Further details on the engine schematic and instrumentation can be found in Fig. 3.

Only the close-coupled section of the exhaust aftertreatment was installed in the testbed due to space constraints. Nevertheless, an exhaust flap (see Fig. 3) was used to replicate the backpressure of the whole line which was obtained from dedicated CFD simulations. The engine was managed by means of two devices, as illustrated in Fig. 4. An ETAS ES910 Rapid Control Prototyping (RCP) module was added to the standard production Engine Control Unit (ECU) of the baseline Stellantis engine to enable the control of the new actuators of the prototype, i.e., the EGR valve and flap, the VNT rack, the E-Turbo, the EHC and the SCR urea injector. Morphee 3 from FEV served as test supervisor, while Osiris from FEV was used for high-frequency data acquisition. Combustion analysis, including heat exchange evaluation, was performed using a dedicated in-house tool developed at IFPEN.

3.2. Investigation methodology

The dual dilution combustion system was tested at the engine test bench under steady-state conditions with the aim to find the best trade-off between maximizing BTE and minimizing engine-out pollutant emissions. The experimental campaign took advantage of the results of a set of sensitivity analyses performed on the main engine parameters through a 1D-CFD digital twin of the PHOENICE prototype developed by the authors in previous project work packages [27,28]. The testing activity was performed on 37 key points, depicted in Fig. 5, which were identified as the most representative of the real-world operation of the engine by preliminary 0D vehicle simulations [9].

The experimental investigation followed an approach made of three sequential steps, each involving variations in key parameters:

I. **Fuel injection**: fuel rail pressure and Start of Injection (SOI)
II. **Intake valves profile and timing**: Intake Valve Opening (IVO) and Intake Valve Closing (IVC) angles
III. **Dual dilution combustion**: Air-Fuel Ratio (AFR) and EGR rate

The optimal combination identified at each step served as the baseline for the subsequent stage of the procedure. Although such an “One Factor At a Time” (OFAT) approach cannot be considered as optimal as pointed-out in [29] since it fails to consider possible interactions between factors, a full factorial or any other Design of Experiment (DoE) approach would not have been practically implementable in this case due to the complexity of the system and limited time available. Therefore, the adopted methodology was the following: first, through the OFAT-based experimental investigation here reported, the main

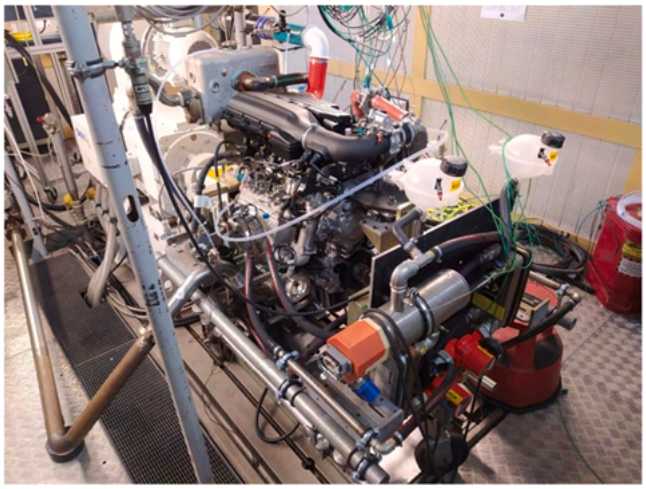

Fig. 2. PHOENICE prototype engine installed on the IFPEN test bench.

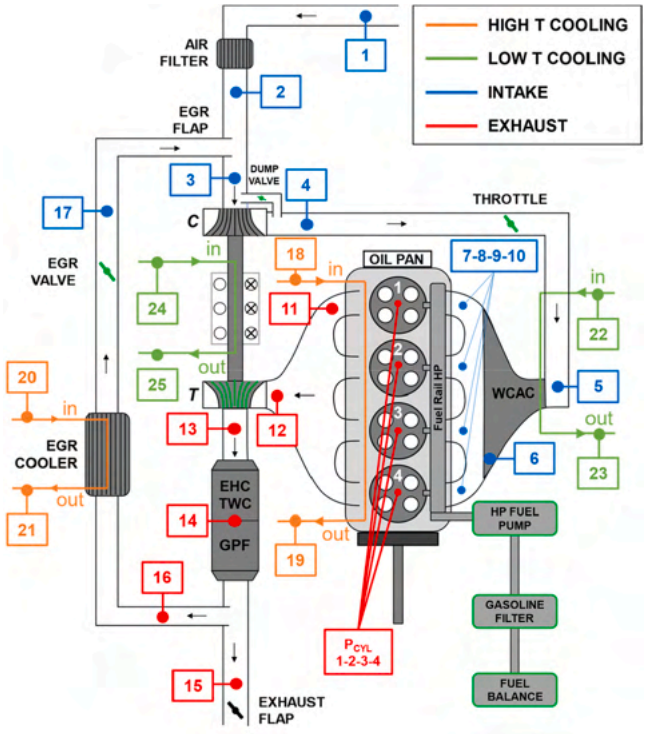

Fig. 3. Engine schematic and instrumentation.

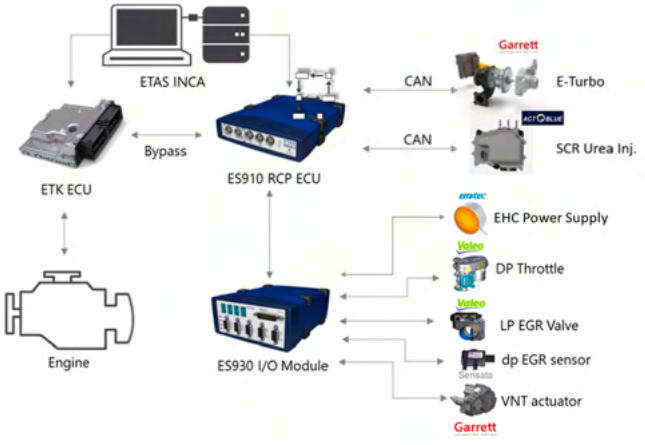

Fig. 4. Engine control system architecture.

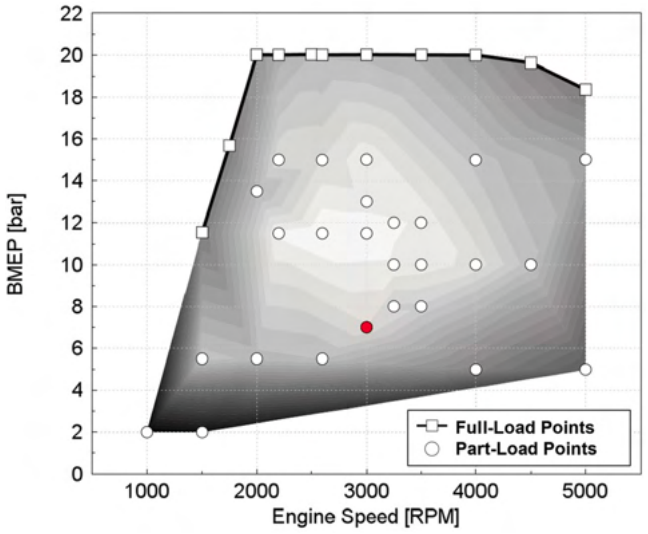

Fig. 5. Engine operating points for steady-state investigation. 3000 RPM x 7.0 bar BMEP is highlighted in red.

sensitivities of BSFC, emissions and combustion stability to different calibration parameters (such as, for instance, injection pressure, SOI, IVO, IVC, etc.), were explored. Then, on the basis of the gathered experimental data, a comprehensive predictive 0D-1D CFD engine model was calibrated as described in [27,28]. Finally, the calibrated and validated model was then exploited to perform a numerical full factorial DoE and identify the optimal engine calibration.

For sake of brevity, in the next paragraphs, only the experimental results obtained with the OFAT methodology for the 3000 RPM x 7.0 bar BMEP operating point (highlighted in red in Fig. 5) will be discussed, since it is the most significant operating point based on the previously mentioned driving cycle simulations [9].

3.2.1. *I step: fuel injection optimization*

Concerning fuel injection, several combinations of SOI timings, ranging between 240 CA and 320 CA before Top Dead Center of firing (bTDCf), and rail pressures, ranging from 200 bar up to 350 bar, were investigated. For all the considered SOI timings, the injection event always occurred during the intake stroke with open intake valves.

Fig. 6 shows the results in terms of BTE, friction losses (FMEP), brake specific CO+HC emissions and Particulate Number (PN) with the star symbol indicating the identified optimal trade-off. Increasing the rail pressure has a slightly negative impact on BTE due to higher engine friction generated by the higher power consumption of the fuel pump. On the other side, PN emissions can be reduced by more than 50 % by raising the rail pressure from 200 bar to 300 bar, with a limited penalty on CO+HC emissions. This is primarily due to improved fuel atomization and a shorter injection duration, which result in better mixture homogeneity. At 350 bars, no further benefits on PN reduction can be observed. The effect of SOI is quite limited. The largest variation was observed at 350 bar, but the optimal value for minimizing PN for all the tested pressure levels is 290 CA bTDCf. Retarding the SOI towards the end of the intake stroke leads to a poorer mixture homogeneity which results in higher PN emissions.

Thus, the optimal injection parameters were found, and a $P_{rail} = 300$ bar and a SOI = 280 CA bTDCf were chosen based on the trade-off between PN and BTE shown in Fig. 7.

3.2.2. *II step: intake valves profiles and timing optimization*

The fully variable valve actuation system of the PHOENICE prototype provides a high flexibility in the optimization of the timing and of the lift profile of the intake valves. It enables aggressive cycle Millerization, which can be realized through either an Early IVC (EIVC) or a

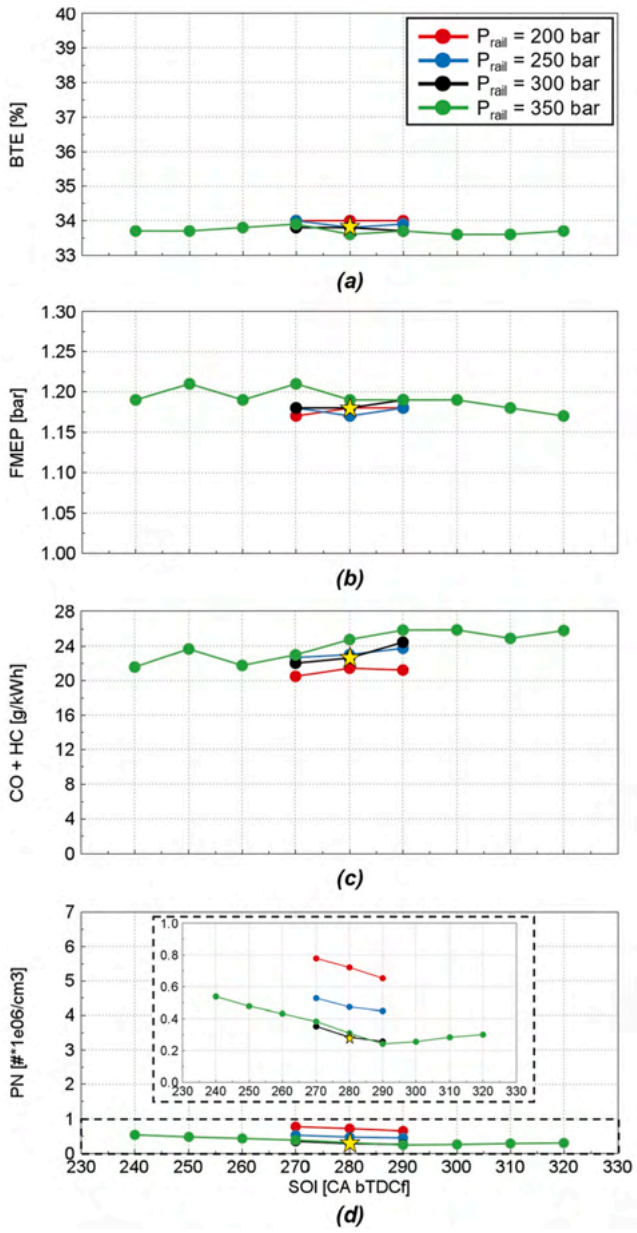

Fig. 6. 3000 RPM x 7.0 bar BMEP – Effects of P_{rail} and SOI on (a) BTE, (b) FMEP, (c) engine-out bsCO + bsHC and (d) engine-out PN. Experimental results.

Late IVC (LIVC) strategy [24].

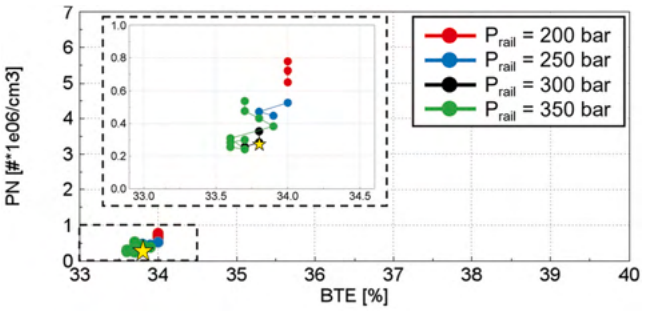

Fig. 7. 3000 RPM x 7.0 bar BMEP – PN / BTE trade-off. Experimental results.

In this step, the best IVO and IVC angles were identified. The former was varied from −10 CA (retard) to +20 CA (advance) with respect to the TDC of gas exchange, while the latter was spanned from 490 to 650 CA after Top Dead Center of Firing (aTDCf). Both opening and closing angles correspond to a lift of 1 mm. Fig. 8 displays the results in terms of BTE, pumping losses (PMEP), combustion phasing (MFB50), NOx and PN emissions. For a given IVO, the benefits of early and late Miller on BTE were found to be comparable. The main factor that drives the efficiency improvement for the considered part load condition is the considerable de-throttling and the consequent reduction of the pumping losses that occurs when the intake valve closing is highly anticipated or retarded. Furthermore, the decreased in-cylinder pressure and temperature at spark ignition reduce the knock tendency caused by the high CR of 13.6. The MFB50 can thus be advanced, achieving a better combustion phasing and a further increase of the engine efficiency. Regardless of the adopted IVO, late Miller provides slightly higher BTE and no penalty on PN emissions thus supporting earlier findings reported in the literature [30]. This slightly higher efficiency gain is due to the reduced power consumption of the VVA system when a LIVC strategy is chosen. In contrast, with an EIVC approach, the energy stored in the valve spring is wasted on pumping the VVA oil into the circuit reservoir [24].

The MultiAir system embeds a peculiar “boot” cam profile that can be actuated by means of very early IVO angles to increase the amount of internal EGR through valve overlap. The resulting effect is clearly visible for IVO +20 CA, as the large amount of residuals left over from the combustion process helps reducing NOx formation. Unfortunately, when early IVO is coupled with early IVC a drastic increase of PN emissions is observed, mostly due to the poor mixture homogeneity caused by the turbulence deterioration associated with early Miller cycles.

Absolute BTE gains of up to 2 % over the previous step were achieved with more than 30 % NOx reduction for IVO of +20 CA and IVC of 620 CA aTDCf. As a result, for this optimization phase, this is the best combination that was selected.

3.2.3. III step: dual dilution combustion optimization

As previously mentioned, the DDCA consists of the synergic use of homogeneous mixture enleanment (relative air-to-fuel ratio $\lambda > 1$) and cooled LP EGR. The potential benefits of this highly diluted combustion mode were thoroughly evaluated by performing several EGR sweeps at increasing λ levels as long as acceptable combustion stability and duration were guaranteed.

Fig. 9 summarizes the outcomes in terms of BTE, pumping losses (PMEP), combustion stability (CoV of IMEP) and CO + HC emissions. Data points falling outside the acceptable CoV of IMEP threshold are represented by hollow circles. As expected, independently from the use of EGR or lean λ, the charge dilution is significantly beneficial for the engine thermal efficiency. Such behavior can be attributed to the decrease of the heat losses generated by the lower combustion temperature. Furthermore, although aggressive cycle Millerization already enables significant de-throttling under stoichiometric conditions, operating the engine in lean mode increases the air demand, leading to a further increase in throttle angle and, consequently, in a further reduction in pumping losses. It should be mentioned that, independently from the EGR level, air dilution improves combustion completeness as well, as seen by the sharp drop in CO+HC emissions at $\lambda > 1$.

The analysis of the emission trends reported in Fig. 10 points out that the EGR is highly effective in reducing in-cylinder NOx formation without significant penalties on PN emissions. The combination of $\lambda = 1.43$ and EGR Rate = 7.0 % was found to be the optimal trade-off, yielding to quite satisfactory results. Specifically, a 3 % increase in BTE coupled with a 50 % decrease in CO + HC emissions, and a more than 60 % reduction in NOx emissions were achieved in comparison to the stoichiometric operation without EGR.

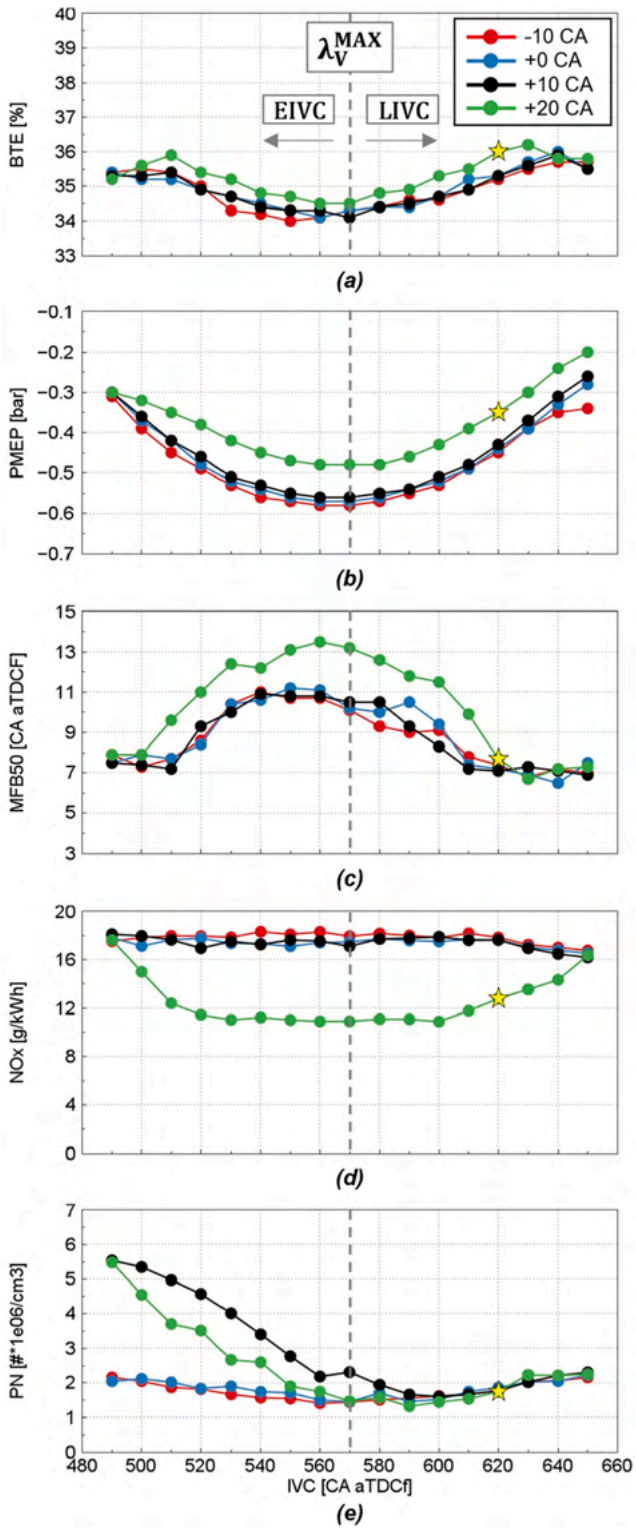

Fig. 8. 3000 RPM x 7.0 bar BMEP - Effects of IVO and IVC on (a) BTE, (b) PMEP, (c) MFB50, (d) engine-out NOx and (e) engine-out PN. Experimental results.

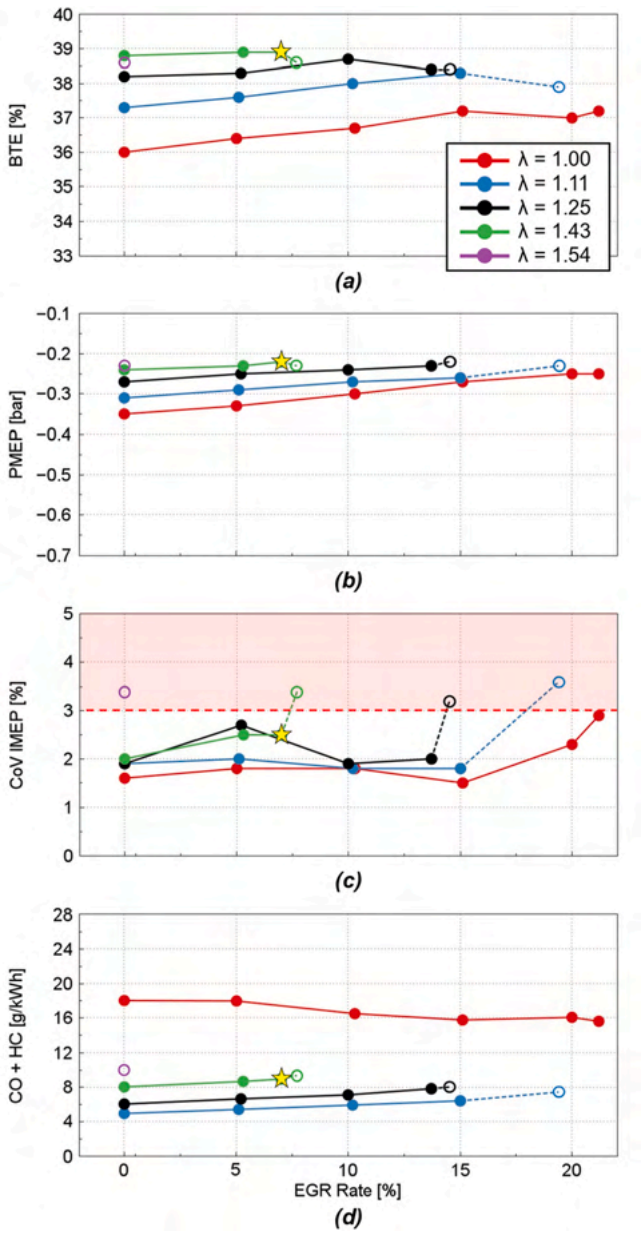

Fig. 9. 3000 RPM x 7.0 bar BMEP – Effects of charge dilution on (a) BTE, (b) PMEP, (c) CoV of IMEP and (d) engine-out bsCO + bsHC. Experimental results.

4. Engine performance assessment

The comprehensive analysis of the trends described in the previous section was applied to the entire test matrix depicted in Fig. 5, leading to the definition of a preliminary engine calibration for three different combustion modes. Indeed, under real driving conditions, the PHOENICE engine is expected to switch among 3 different combustion modes according to its thermal state and to the temperature of the aftertreatment. In particular, it can operate at:

- $\lambda = 1$ without EGR when the engine coolant temperature is below 75 °C
- $\lambda = 1$ with EGR when the target coolant temperature is achieved
- $\lambda > 1$ with EGR when the target coolant temperature is achieved, and the SCR is in the temperature window of maximum conversion efficiency

In what follows, the impact of the PHOENICE technologies on both thermal efficiency and pollutant emissions will be assessed considering the whole engine map. To highlight each contribution, the combustion modes will be separately analyzed. First, the results achieved in stoichiometric operation will be presented to point out the benefits of the high CR and cycle Millerization. Next, the efficiency gains obtained through the use of the EGR will be analyzed. Finally, the effects of dual

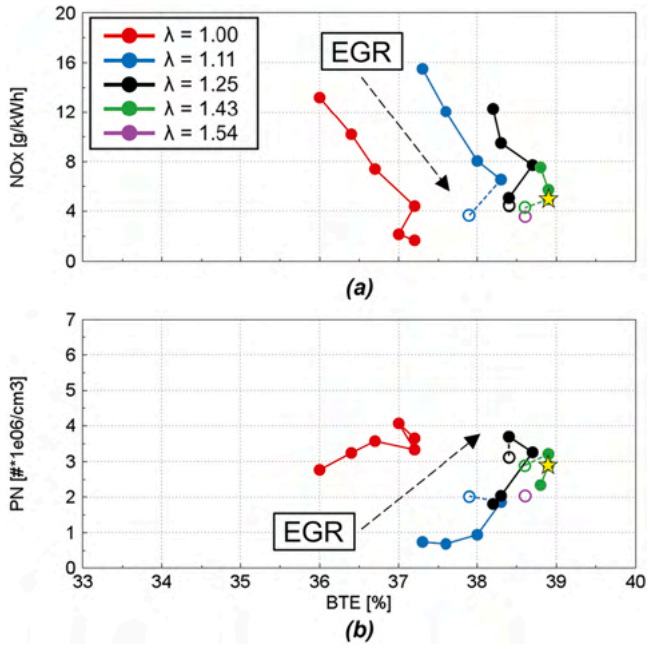

Fig. 10. 3000 RPM x 7.0 bar BMEP – (a) NOx / BTE trade-off and (b) PN / BTE trade-off. Experimental results.

dilution combustion will be illustrated, with a focus on the improvements achieved over the reference base engine.

4.1. Effects of high CR and miller cycle

The high CR is the main responsible for the high BTE at low loads, while the late Miller strategy, which was extended throughout the entire operating map, is effective at high loads (see Fig. 11). Indeed, the reduction of the effective compression ratio leads to a lower knock likelihood, and to an improvement of the combustion phasing. Moreover, the higher boost pressure required for LIVC operation is provided by the optimized design of the compressor wheel of the E-Turbocharger. However, below 2000 RPM, aggressive use of LIVC is constrained by the compressor surge limit. Finally, the VVA has a non-trivial contribution also at low load where the use of a retarded IVC enables a reduction of the pumping losses thanks to the engine de-throttling.

4.2. Effects of cooled LP EGR

Fig. 12 shows the optimal EGR map under stoichiometric conditions and the corresponding BTE improvement. The maximum recirculation level is about 20 % and its effects are more relevant at medium loads, i.e., 5.0 bar < BMEP < 15.0 bar, where a maximum relative gain of about 4.2 % was achieved. In fact, in that BMEP range, besides the reduction of the heat losses, the knock suppression capabilities of the EGR improve the combustion phasing which, in turn, offsets the increase in the exhaust back pressure related to the use of high recirculation rates. On the other side, above 15.0 bar BMEP, the use of EGR has to be limited because of additional constraints on the compressor surge, on the pressure at the turbine inlet and on maximum in-cylinder pressure, which was already increased by the use of Miller Cycle and high CR. Therefore, in these conditions, an increase of the BTE was not possible since there is a unique solution to limit the knock occurrence: the use of a more retarded combustion.

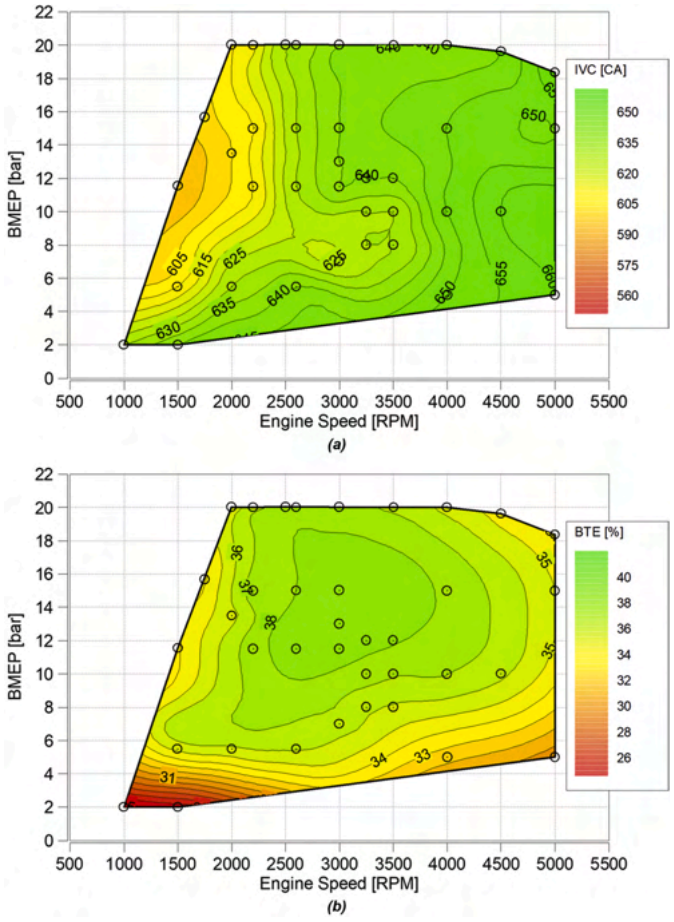

Fig. 11. (a) Optimized IVC map for late Miller cycle at λ = 1 without EGR and (b) BTE. Experimental results.

4.3. Effects of dual dilution combustion

As shown in Fig. 13(b), the enleanment of the mixture allowed improving the BTE of the λ = 1 + EGR combustion mode up to 5 %. It is worth underlining that the optimal EGR rate in lean conditions is different from the EGR rate under stoichiometric operation.

As noticeable in Fig. 13(a), lean mapping is adopted up to 13.0 bar BMEP while at higher load the engine operates in stoichiometric conditions using EGR to limit the occurrence of abnormal combustion phenomena. In those operating conditions, indeed, the increase of the AFR did not enable further efficiency improvements but led to higher NOx emissions. The region between 3000 RPM and 4000 RPM and between 7.0 bar and 10.0 bar BMEP is characterized by the highest air dilution rates. For the BTE, a maximum relative improvement of 4.6 % was obtained at 3000 RPM and 8.0 bar BMEP. The use of ultra-lean mixture greatly improves combustion efficiency through a substantial reduction of heat losses. As a matter of fact, as illustrated by Fig. 14(a), a wide portion of the engine operating map is characterized by a gross ITE above 45 % with a peak close to 47 % at 3500 RPM and 8.0 bar BMEP which matches the target of the project. In the same area, the BTE exceeds 38 % (see Fig. 14(c)) with a maximum value approaching 41 % at 3000 RPM and 11.5 bar BMEP. A stable combustion process is guaranteed by the strong charge motion generated by the Swumble™. Indeed, the detrimental effects that the mixture dilution has on the flame propagation speed and on the cycle-to-cycle variability are effectively counteracted, resulting in a satisfactory combustion duration

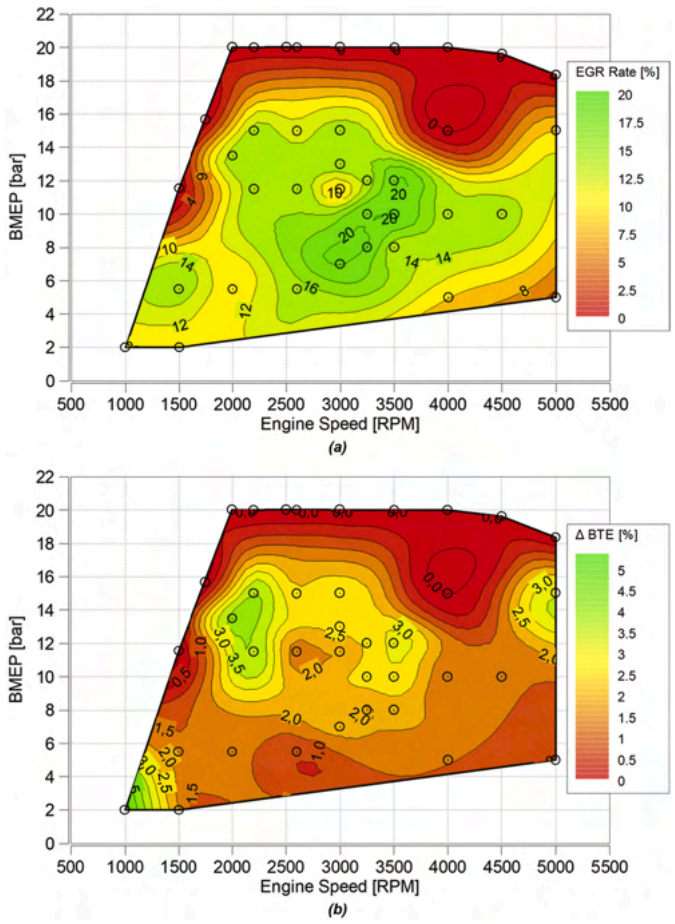

Fig. 12. (a) Optimized EGR rate at $\lambda = 1$ and (b) relative improvement on BTE with respect to $\lambda = 1$. Experimental results.

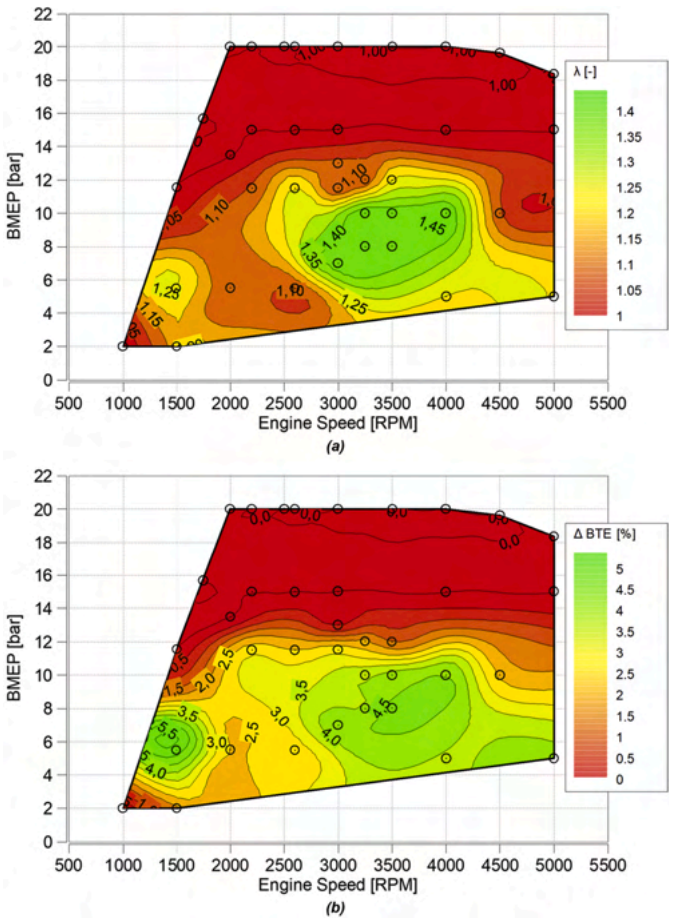

Fig. 13. (a) Optimized air dilution map (λ) and (b) relative improvement on BTE with respect to $\lambda = 1$ with external LP EGR. Experimental results.

(BD10–90), as demonstrated by Fig. 14(d).

A benchmark of these results against the base engine reveals significant improvements of the BTE efficiency, as illustrated in Fig. 15. For a large portion of the map, especially at partial loads, these improvements are greater than 10 %, proving the fuel economy potential of the PHOENICE engine concept. As already discussed, most of the contribution derives from the synergic use of the high CR, of aggressive cycle Millerization and of dual charge dilution. Only at full load the efficiency levels are comparable. In fact, between 1500 and 2000 RPM, the compressor surge as well as the lack of enthalpy within the turbine limit the use of the VVA forcing, at the same time, the adoption of a very retarded combustion to reduce the knock likelihood (see Fig. 14(b)). However, since the PHOENICE engine concept is integrated in a plug-in hybrid electric vehicle, the operation within this area could be prevented through suitable exploitation of the electric machines. No benefits are observed above 3000 RPM either, due to the significantly higher exhaust backpressure caused by the complex aftertreatment system configuration which leads to an increase of the pumping losses.

Besides the BTE improvements, it is of paramount importance to analyze the variation of the pollutant emissions which, according to the project targets, must comply with the upcoming EU7 regulation.

Fig. 16(a) points out that carbon monoxide emissions are noticeably low under part load operation, especially in the region characterized by the leanest λ values. This indicates that the combustion system operates efficiently, enabling near-complete combustion and significantly reducing CO emissions. Only at 1500 RPM, when the full load curve is reached, a peak of carbon monoxide can be observed. It is related to the presence of a retarded split injection strategy which is used to suppress the knock occurrence. The good combustion stability and completeness can be also proved by the analysis of unburned hydrocarbons depicted in Fig. 16(b), which are quite low across almost the entire engine operating map. As expected, the air dilution poses great challenges for the nitrogen oxides abatement. Fig. 16(c) demonstrates that up to 3000 RPM, NOx emissions are quite low mainly because of the extensive use of EGR, which reduces the temperatures and the oxygen concentration in the combustion chamber. However, above this speed, the reduction of the EGR rate leads to an increase of the NOx emissions. Such behavior underlines the need for a tradeoff between the charge dilution for optimal thermal efficiency and for minimum NOx production. Finally, the particulate matter emissions, measured through its number of particles (PN) and expressed in millions per cubic centimeter, are shown in Fig. 16(d). The highest emissions are observed at high speeds and low loads. As previously discussed, in this region the engine operates with a high valve overlap to reduce both the pumping losses and the NOx emissions through the increase of the internal EGR. However, the backflow of the residual gases into the intake manifold may disrupt the internal aerodynamics affecting mixture homogeneity and, consequently, leading to higher particulate matter formation.

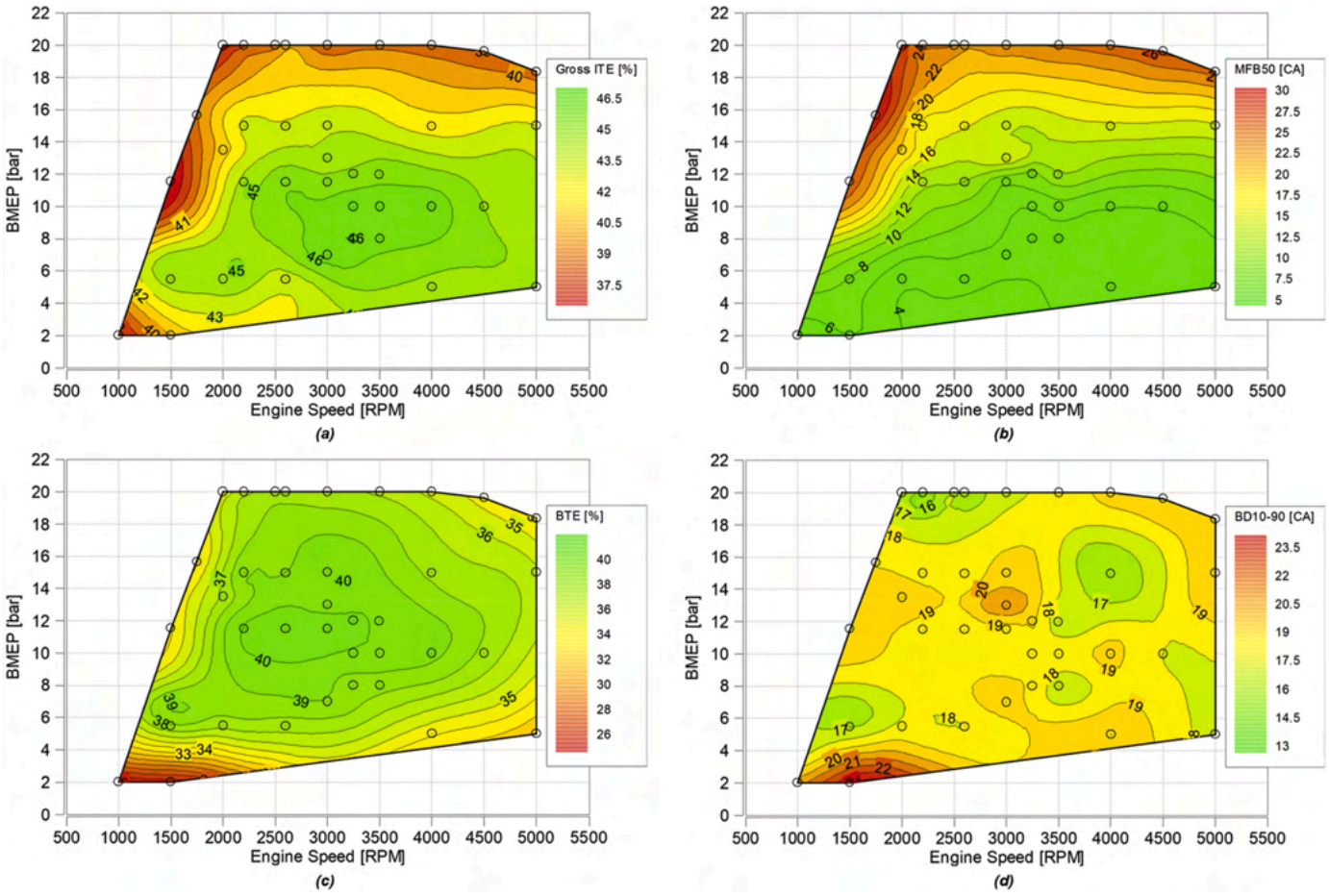

Fig. 14. (a) Gross Indicated Thermal Efficiency, (b) Brake Thermal Efficiency, (c) combustion phasing (MFB50) and (d) combustion duration (BD10–90). Experimental results.

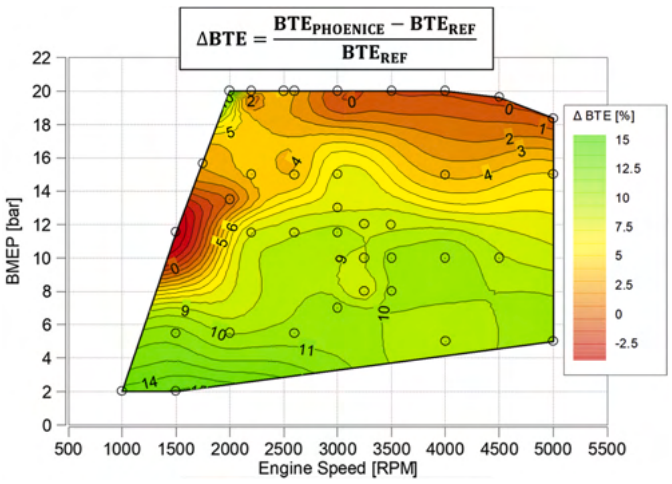

Fig. 15. Relative improvement in BTE in comparison with the baseline engine. Experimental results.

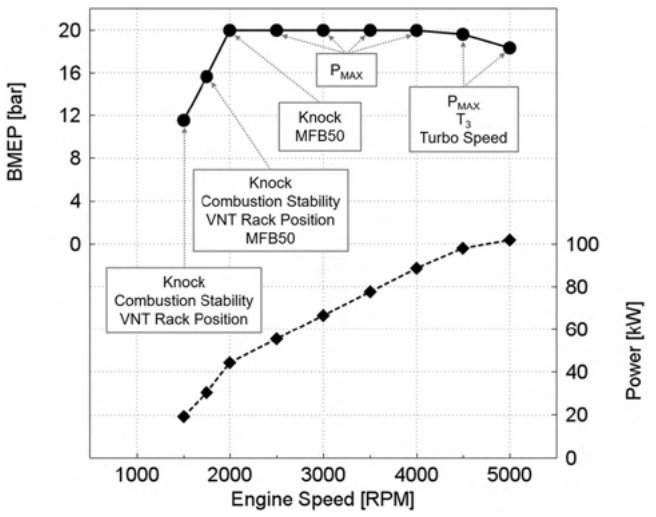

Fig. 17. PHOENICE full load curve showing main limiting factors.

4.4. *Full load performance*

As shown in Fig. 17, the engine successfully met the project targets, achieving a maximum BMEP of 20.0 bar between 2000 and 4000 RPM, and a rated power of 100 kW at about 5000 RPM.

Below 2000 RPM, the engine performance reflects the trade-off among knock severity, combustion stability, and boost requirements. As previously mentioned in Section 4.1, in this region, intense use of LIVC is not possible because of the limitations of the charging system.

Between 2500 and 4000 RPM, the combustion phasing can be advanced thanks to the high limit on maximum in-cylinder pressure (P_{MAX}). This constraint incorporates a 3-sigma margin relative to the average peak in-cylinder pressure to ensure that safe engine operations are maintained, even when accounting for cycle-to-cycle pressure fluctuations. At 4500 and 5000 RPM, the main constraints on the engine performance are the maximum turbo speed, the turbine inlet temperature T_3 and the P_{MAX}.

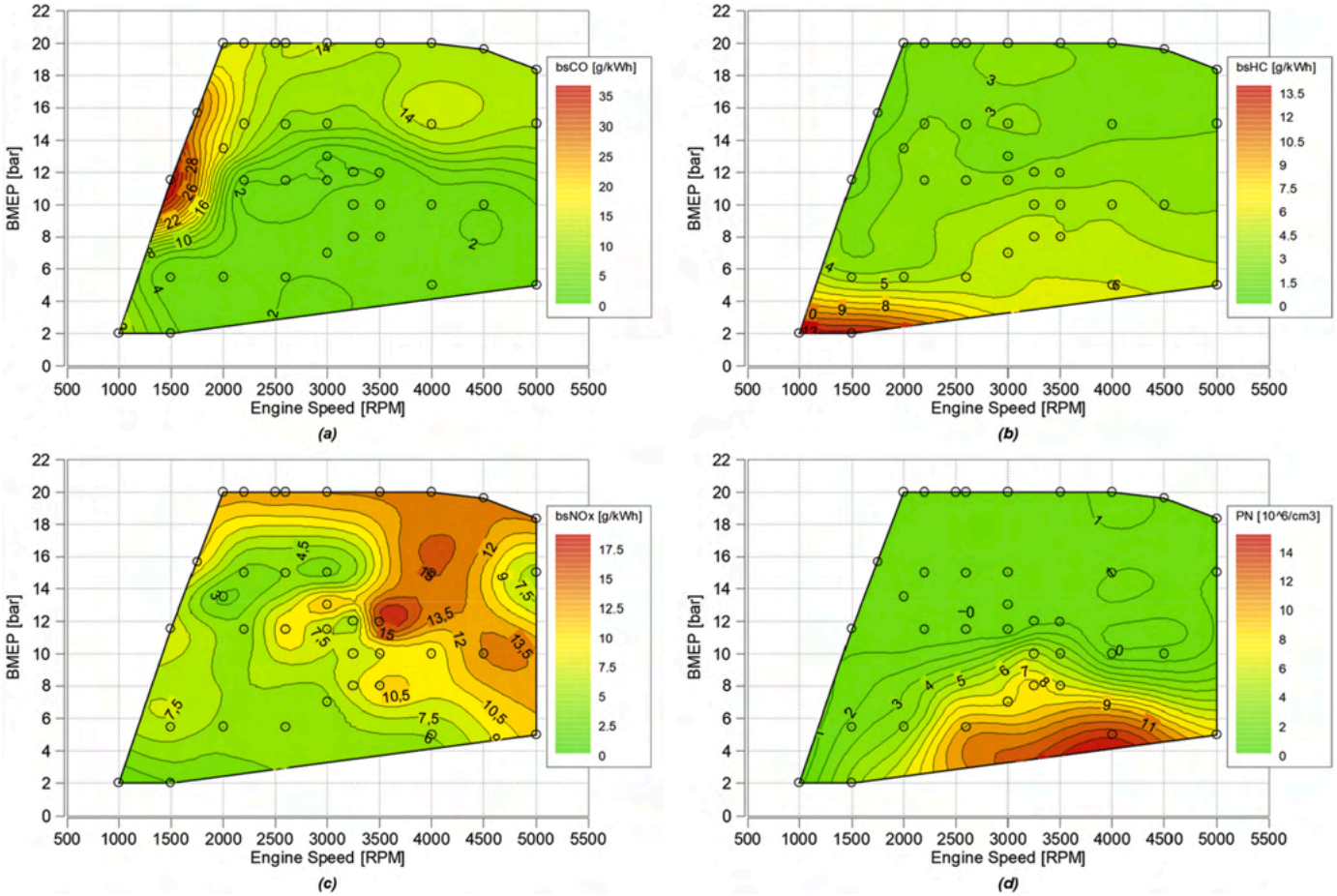

Fig. 16. Engine-Out pollutant emissions maps: (a) CO emissions, (b) HC emissions, (c) NOx emissions, (d) particle number emissions. Experimental results.

5. E85: further potential of renewable fuel

Additional tests were also conducted to assess the potential of alternative fuels featuring a reduced environmental impact. In particular, a blend consisting of 85 % bioethanol and 15 % pure gasoline (i.e., E85) was considered in this study. Table 2 compares its properties against the standard E10 gasoline (10 % of ethanol content) used for the engine calibration and highlights a significantly higher Research Octane Number (RON), an inferior Lower Heating Value (LHV), a higher latent heat of vaporization and a lower stoichiometric AFR.

The impact of E85 was evaluated on a reduced number of engine operating points in the central region of the test matrix shown in Fig. 5 and in the dual dilution combustion mode. The tests followed a "drop-in" scenario, where the engine calibration defined for E10 fuel (i.e., fuel injection strategy, intake valves profiles, λ and EGR rate) was kept unchanged while only the spark timing was adjusted to account for the different combustion characteristics of E85.

Table 2
E10 and E85 fuel properties.

	Unit	E10	E85
C Content	% m/m	83.0	57.0
H Content	% m/m	13.5	13.2
O Content	% m/m	3.5	29.8
Density @ 15 °C	kg/m^3	745.3	786.0
RON	–	96.6	106.0
LHV	MJ/kg	41.51	29.07
Latent Heat of Vaporization	kJ/kg	390–410	700–780
Stoichiometric AFR	–	14.01	9.80

Fig. 18 presents the BTE of the engine running on E85, along with its relative improvement with respect to the E10 reference, the new combustion phasing, and the burn duration. E85 demonstrated a better MFB50 and a shorter BD10–90, resulting in a maximum BTE of nearly 42 % at 3000 RPM and 13.0 bar BMEP, representing a relative 5.3 % increase over E10. The largest benefits were observed in the low-end torque region, where relative efficiency gains of up to 16 % were achieved. Under these operating conditions, indeed, E85 significantly mitigates knock due to its high RON, elevated heat of vaporization, and the increased injected mass necessary to compensate for its lower LHV. Furthermore, the lower stoichiometric AFR of E85 resulted in a substantial reduction in boost pressure demand, which in turn reduced pumping losses, further improving efficiency. On the other hand, at part-load, only modest increases of BTE were observed, primarily driven by reduced heat losses. These findings demonstrate that the favorable thermodynamic properties of E85 complement its CO_2 reduction potential by further raising fuel conversion efficiency, confirming earlier results of previous studies [21].

Fig. 19 shows the relative differences in pollutant emissions, where positive values indicate higher pollutant emissions with E85. A slight increase in carbon monoxide emissions was observed across all test points, likely due to worse mixture homogeneity caused by the enhanced cooling effect from ethanol evaporation. Unburnt hydrocarbons were also higher due to the lower LHV, which increases the injected fuel quantity and, consequently, the mass trapped in crevices and wall wetting. Conversely, the reduction of in-cylinder temperatures enabled

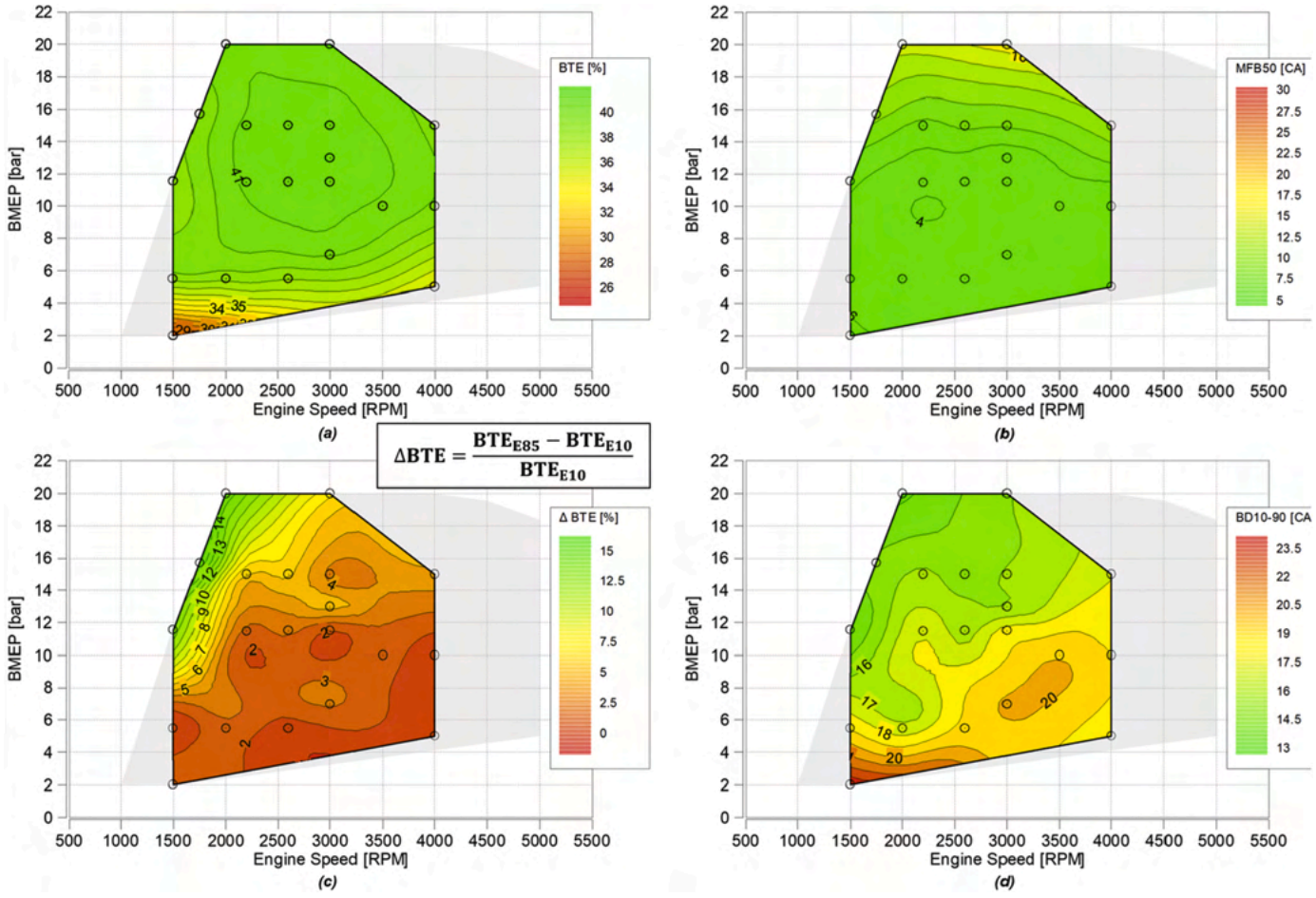

Fig. 18. E85 results: (a) Brake Thermal Efficiency, (b) combustion phasing (MFB50), (c) relative BTE improvement vs E10 and (d) combustion duration (BD10–90). Experimental results.

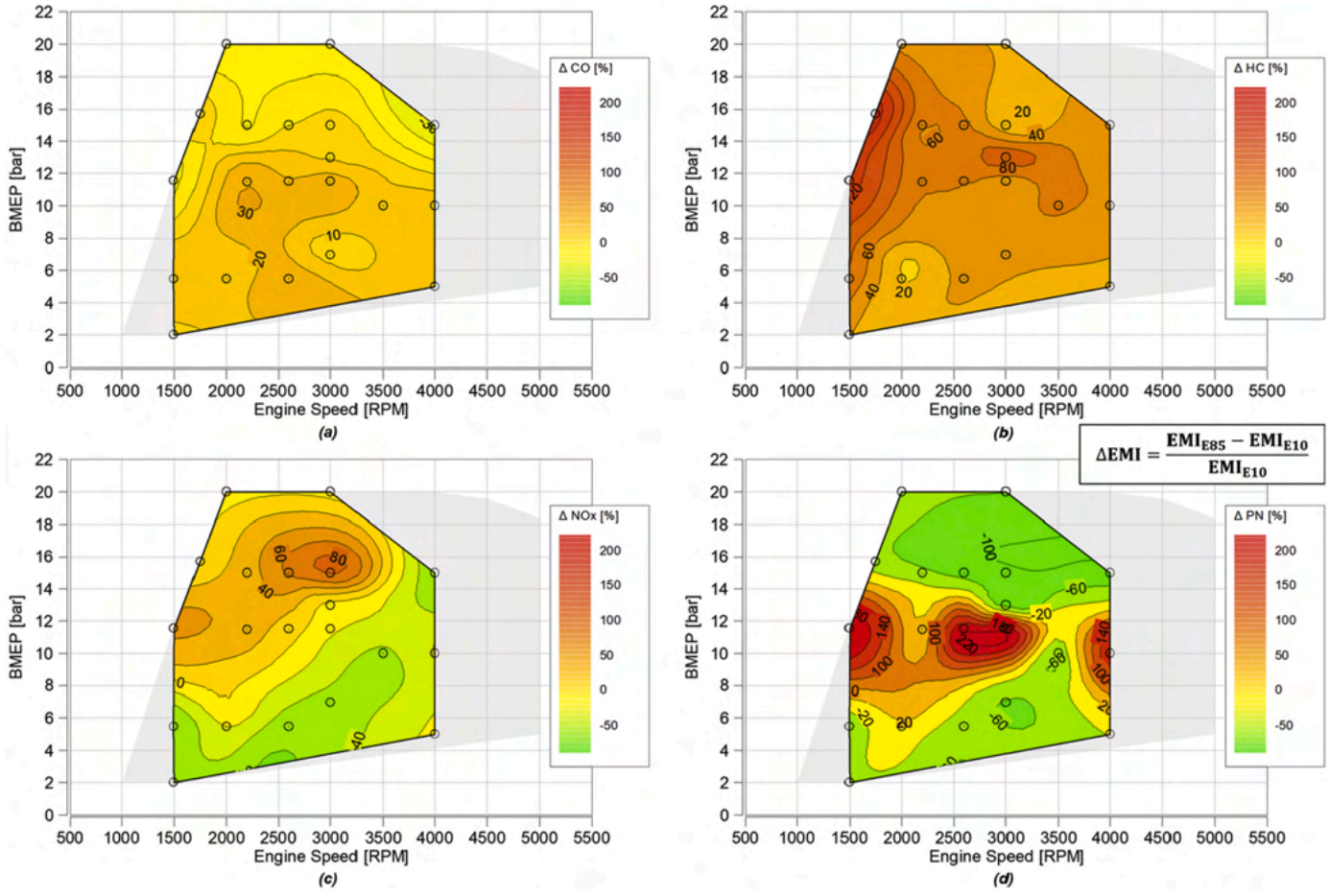

Fig. 19. Engine-Out pollutant emissions difference between E10 and E85: (a) CO emissions, (b) HC emissions, (c) NOx emissions, (d) PN emissions. Experimental results.

by E85 is highly beneficial for NOx emissions up to 10.0 bar BMEP. However, at higher loads, this trend reverses, as improved combustion phasing leads to higher combustion temperatures. Although ethanol contains significantly lower concentrations of aromatic hydrocarbons, which are known precursors to particulate matter formation during combustion, an analysis of particulate emissions does not reveal a consistent trend. Nevertheless, it is important to emphasize that, in absolute terms, the emissions remain relatively low, indicating that the observed variations may not have substantial relevance.

The advantageous properties of E85 also enable an improvement of the engine performance, particularly at low engine speeds. Fig. 20 compares the full load curves achieved with E10 and E85, respectively. The latter shows a better combustion stability, a better combustion phasing, and a lower boost pressure. For such reasons it was possible to extend the 20.0 bar BMEP target down to 1500 RPM and to slightly improve the rated power at 4500 RPM.

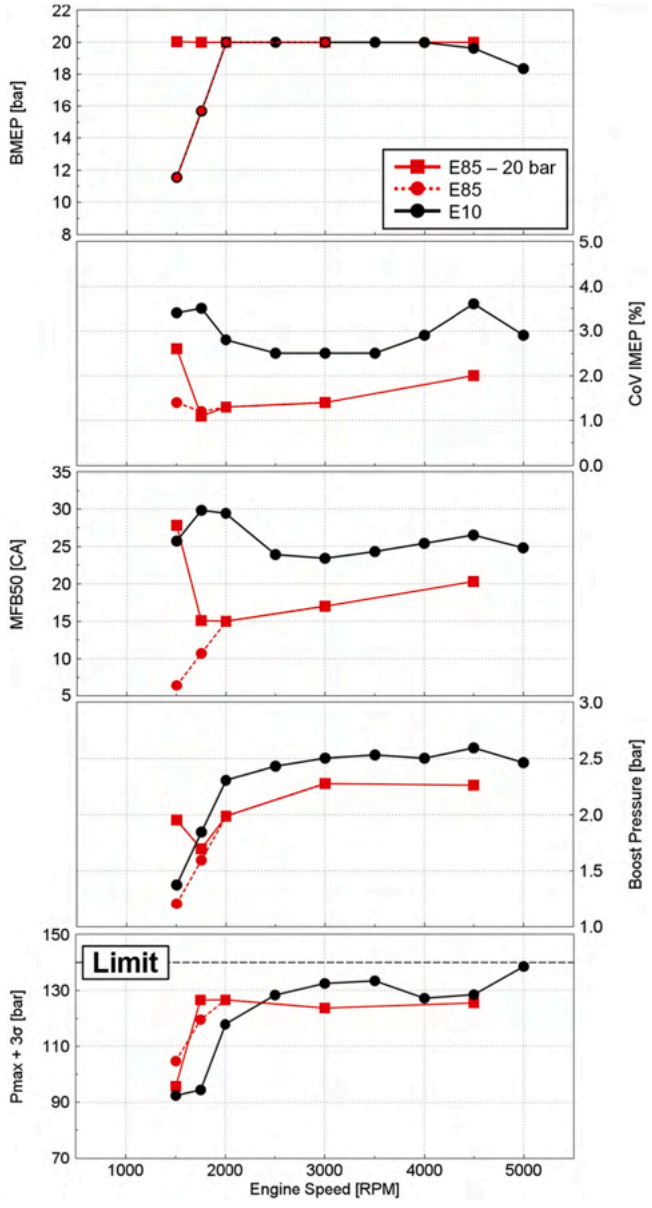

Fig. 20. Comparison of full load engine parameters with E85 and with E10. Experimental results.

6. Conclusions

This study, developed in the framework of the H2020 PHOENICE project, proved the potential to strongly reduce the environmental impact of the next generation of SI engines through a synergic use of highly innovative technologies. The proposed concept, based on a 1.3L state-of-the-art Stellantis engine, features an extremely high compression ratio to improve energy conversion efficiency at part load. At higher BMEP levels, a proper combination of EGR and aggressive cycle Millerization was employed to limit the knock occurrence. Further benefits in both CO_2 and pollutant emissions were achieved through a highly diluted combustion process, which leverages innovative in-cylinder charge motion to maintain acceptable combustion stability, alongside a redesigned VNT turbocharger to meet the increased boost pressure requirements.

An extensive experimental campaign was carried out in steady-state conditions at the engine test rig to assess the synergistic potential of the implemented technologies for such a complex prototype. A sequential process was followed focusing on sensitivity analyses on the fuel injection system, of the variable intake valve actuation and of the dual charge dilution. As expected, the high compression ratio was very effective at low loads, where BTE never drops below 30 %. The cycle Millerization was beneficial throughout the whole engine map, since it limited the knock occurrence and reduced the pumping losses at high and low loads, respectively. As a result, in stoichiometric conditions, the PHOENICE engine was able to achieve a maximum BTE of about 38 % with a wide region above 34 %. The introduction of the EGR enabled a further relative improvement of about 4.2 % in BTE, thanks to the reduction in the heat losses and of the knock likelihood. Nevertheless, above 15.0 bar BMEP, the EGR levels had to be limited because of additional constraints on the compressor surge, on the pressure at the turbine inlet and on the maximum in-cylinder pressure. Concerning the mixture enleanment, the region between 3000 and 4000 RPM and between 7.0 bar and 10.0 bar BMEP showed the highest dilution rates and a further maximum relative increase in BTE of 4.6 %, primarily due to a substantial reduction in heat losses. Moreover, a wide portion of the engine operating map is characterized by a gross ITE above 45 % with a peak close to 47 % at 3500 RPM and 8.0 bar BMEP, which matches the target of the project. Compared to the base engine, the PHOENICE concept achieved improvements greater than 10 % in BTE over a wide region of the operating map. Remarkable results were also achieved from the pollutant emissions perspective. As a matter of fact, extremely low emission levels were observed for both CO and NOx. However, at high load, the NOx production rate rose because of the high in-cylinder temperature and of the limited EGR levels. Regarding particulate matter, the use of lean combustion resulted in minimized emissions levels, even down to 10nm, showing promising results in relation to the upcoming EU7 limits. Only at high speeds and low loads, the high valve overlap led to mixture inhomogeneities which could negatively affect the PM formation. Finally, this study pointed out the additional benefits which can be obtained on energy conversion efficiency through the use of a renewable fuel. The PHOENICE concept, indeed, when operated with E85 using the same engine calibration optimized for E10, showed a maximum BTE increase of 16 %, even if with higher pollutant emissions.

Future steps of the project will concentrate on refining the engine calibration for transient conditions, integrating it into the vehicle prototype, and assessing its fuel economy potential in both regulatory driving cycles and real-world driving conditions.

CRediT authorship contribution statement

Toni Tahtouh: Writing – review & editing, Supervision, Project administration, Methodology, Funding acquisition, Formal analysis, Conceptualization. **Mathieu André:** Methodology, Investigation, Formal analysis. **Giuseppe Castellano:** Writing – original draft, Formal analysis, Data curation. **Luciano Rolando:** Writing – review & editing,

Supervision, Formal analysis. **Federico Millo:** Writing – review & editing, Supervision, Project administration.

Declaration of competing interest

The authors declare the following financial interests/personal relationships which may be considered as potential competing interests:

Toni Tahtouh reports financial support was provided by European Commission. If there are other authors, they declare that they have no known competing financial interests or personal relationships that could have appeared to influence the work reported in this paper.

Acknowledgments

This project has received funding form the European Union's Horizon 2020 research and innovation program under Grant Agreement No. 101006841.

Data availability

The data that has been used is confidential.

References

[1] European Parliament Press Release: https://www.europarl.europa.eu/news/en/press-room/20230210IPR74715/fit-for-55-zero-co2-emissions-for-new-cars-and-vans-in-2035 (accessed on 17th October 2024).
[2] M. Ovaere, S. Proost, Cost-effective reduction of fossil energy use in the European transport sector: an assessment of the Fit for 55 package, Energy Policy 168 (2022), https://doi.org/10.1016/j.enpol.2022.113085.
[3] Z. Samaras, A. Kontses, A. Dimaratos, D. Kontses, et al., A European regulatory perspective towards a euro 7 proposal, SAE Int. J. Adv. Curr. Prac. Mobility 5 (3) (2023) 998–1011, https://doi.org/10.4271/2022-37-0032.
[4] The European Parliament and the Council of The European Union, "Regulation (EU) 2024/1257 of the European Parliament and of the Council of 24 April 2024 on type-approval of motor vehicles and engines and of systems, components and separate technical units intended for such vehicles, with respect to their emissions and battery durability (Euro 7)," 24 April 2024, https://data.europa.eu/eli/reg/2024/1257/oj (accessed on 17th October 2024).
[5] U. Kramer, D. Bothe, F. Dünnebeil, FVV fuels study IV – Transformation of European mobility to the GHG neutral post-fossil age, Internationaler Motorenkongress (2022) 81–94, https://doi.org/10.1007/978-3-658-44740-3_6.
[6] S. Hartung, Powertrains of the future - how we will meet our climate goals through technology neutrality, 42nd International Vienna Motor Symposium, Vienna (2021), 29-30 April.
[7] Tahtouh, T., Millo, F., Rolando, L., Castellano, G. et al., "A synergic use of innovative technologies for the next generation of high efficiency internal combustion engines for PHEVs: the PHOENICE Project," SAE Technical Paper 2023-01-0224, 2023, https://doi.org/10.4271/2023-01-0224.
[8] PHOENICE project website: https://phoenice.eu/(accessed on 17th October 2024).
[9] T. Tahtouh, M. Brignone, J. Gareth, N. Demeilliers, et al., The PHOENICE Project: a synergic use of innovative technologies for the next generation of green hybrid powertrains, in: 44th International Vienna Motor Symposium, Vienna, 28 April 2023, p. 26.
[10] Y. He, J. Liu, D. Sun, B. Zhu, Development of an aggressive Miller Cycle engine with extended late-intake-valve-closing and a two-stage turbocharger, Proceed. Institut. Mechan. Engineers, Part D 233 (2) (2019) 413–426, https://doi.org/10.1177/0954407017745220.
[11] S. Meng, Z. Han, B. Fan, Z. Wu, Impacts of fuelling methods on knock-limited combustion and emissions of a dedicated hybrid spark-ignition engine, Appl. Thermal Eng. 254 (2024), https://doi.org/10.1016/j.applthermaleng.2024.123898.
[12] Osborne, R., Lane, A., Turner, N., Geddes, J. et al., "A new generation lean gasoline engine for premium vehicle CO2 reduction," SAE Technical Paper 2021-01-0637, 2021, https://doi.org/10.4271/2021-01-0637.
[13] S. Martinez, A. Irimescu, S.S. Merola, P. Lacava, et al., Flame front propagation in an optical GDI engine under stoichiometric and lean burn conditions, Energies 10 (9) (2017) 1337, https://doi.org/10.3390/en10091337.
[14] C. Tornatore, F. Bozza, V. Bellis, L. de Teodosio, et al., Experimental and numerical study on the influence of cooled EGR on knock tendency, performance and emissions of a downsized spark-ignition engine, Energy 172 (2019) 968–976, https://doi.org/10.1016/j.energy.2019.02.031.
[15] Cordier, M., Laget, O., Duffour, F., Gautrot, X. et al., "Increasing modern spark ignition engine efficiency: a comprehension study of high CR and atkinson cycle," SAE Technical Paper 2016-01-2172, 2016, https://doi.org/10.4271/2016-01-2172.
[16] X. Gautrot, M. Bardi, T. Leroy, P. Luca, et al., Swumble™ In-cylinder fluid motion for high efficiency gasoline SI engines: development of the second generation, in: Proceedings of the SIA Powertrain and Electronics, Rouen, 2020, 16-29 November.
[17] G. Bourhis, O. Laget, R. Kumar, X. Gautrot, Swumble In-cylinder fluid motion: a pathway to high efficiency gasoline SI engines, 27th Aachen Colloquium Automobile Engine Technol., Aachen (2018), 8-10 October.
[18] H. Köten, Y. Karagöz, Ö. Balcı, Effect of different levels of ethanol addition on performance, emission, and combustion characteristics of a gasoline engine, Adv. Mechan. Eng. 12 (7) (2020), https://doi.org/10.1177/1687814020943356.
[19] R. Farzam, B. Jafari, F. Kalaki, Turbocharged spark-ignition engine performance prediction in various inlet charged air temperatures fueled with gasoline–Ethanol blends, Int. J. Engine Res. 22 (7) (2021) 2233–2243, https://doi.org/10.1177/1468087420931718.
[20] R. Singh, T. Han, M. Fatouraie, A. Mansfield, et al., Influence of fuel injection strategies on efficiency and particulate emissions of gasoline and ethanol blends In A turbocharged multi-cylinder direct injection engine, Int. J. Engine Res. 22 (1) (2021) 152–164, https://doi.org/10.1177/1468087419838393.
[21] G. Lavoie, R. Middleton, J. Martz, P. Blumberg, Knock and Knock intensity models for boosted SI conditions with gasoline-ethanol blends, Int. J. Engine Res. 24 (2) (2023) 521–535, https://doi.org/10.1177/14680874211055351.
[22] H. Krämer, M. Send, Using drop-In gasolines with increased renewable potential: a comparison to some typical fossil fuels concerning emission testing and fuel composition, 11th Int. Engine Congress (2024). Baden-Baden, 27-28 February.
[23] C. De Marino, G. Maiorana, P. Pallotti, S. Quinto, et al., The Global small engine 3 and 4 cylinder turbo: the new FCA's Family of small high-tech gasoline engines, in: 39th International Vienna Motor Symposium, Vienna, 27 April 2018, p. 26.
[24] L. Bernard, A. Ferrari, D. Micelli, A. Peretto, et al., Electro-hydraulic valve control with MultiAir Technology, MTZ Worldw 70 (2009) 4–10, https://doi.org/10.1007/BF03226988.
[25] Castellanos, J.S., Bontemps, N., André, M. and Rolando, L., "Project PHOENICE and the role of an E-Turbo in a high efficiency PHEV," ATK Dresden, Germany, 26th September 2023.
[26] T. Tahtouh, G. Lucignano, F. Bocchieri, J.S. Castellanos, et al., A methodology to develop a sustainable, high efficiency hybrid propulsion system: the PHOENICE Project, in: Proceedings of the FISITA 2023 World Congress, FWC2023-PPE-051, Barcelona, 2023. https://doi.org/10.46720/FWC2023-PPE-051, 12 –14 September.
[27] Tahtouh, T., Andre, M., Millo, F., Rolando, L. et al., "Development of a digital twin to support the calibration of a highly efficient spark ignition engine," SAE Technical Paper 2023-01-1215, 2023, https://doi.org/10.4271/2023-01-1215.
[28] Rolando, L., Millo, F., Castellano, G., Tahtouh, T. et al., "A numerical model for the virtual calibration of a highly efficient spark ignition engine," SAE Technical Paper 2023-32-0059, 2023, https://doi.org/10.4271/2023-32-0059.
[29] Montgomery, D.C., "Design and analysis of experiments, 10th Edition," John Wiley & Sons Inc., ISBN 9781119492443, 2019.
[30] Luisi, S., Doria, V., Stroppiana, A., Millo, F. et al., "Experimental investigation on early and late intake valve closures for knock mitigation through Miller cycle in a downsized turbocharged engine," SAE Technical Paper 2015-01-0760, 2015, https://doi.org/10.4271/2015-01-0760.